Stark and Zeeman effects in ethylene observed by sub-Doppler infrared spectroscopy

Yit-Tsong Chen and Takeshi Oka
Department of Chemistry and Department of Astronomy and Astrophysics, The University of Chicago, Chicago, Illinois 60637

(Received 8 December 1987; accepted 19 January 1988)

The recent development of sub-Doppler spectroscopy using microwave modulation sidebands on CO_2 laser radiation has enabled us to perform ultrahigh resolution tunable infrared spectroscopy and study the Stark and Zeeman effects in ethylene. Clear Stark splittings were observed in low J vibration–rotation transitions of the ν_7 band by applying an electric field of up to 50 kV/cm. The Stark shift is caused by the polarizability of ethylene as well as by the second order Stark effect between the accidentally degenerate ν_7 and ν_8 vibrational states ($\nu_7^0 - \nu_8^0 = 8.91\ \mathrm{cm}^{-1}$). Analysis of the observed Stark patterns gives the polarizability anisotropies for the ground state to be $\alpha_{aa} - \frac{1}{2}(\alpha_{bb} + \alpha_{cc}) = 1.91(13)$ Å^3 and $\alpha_{bb} - \alpha_{cc} = 0.07(19)$ Å^3 and for the ν_7 state to be $\alpha_{aa} - \frac{1}{2}(\alpha_{bb} + \alpha_{cc}) = 1.78(11)$ Å^3 and $\alpha_{bb} - \alpha_{cc} = 0.15(14)$ Å^3. The dipole moment along the a axis of ethylene induced by the ν_7 and ν_8 vibrations was determined to be $\partial^2\mu_a/\partial q_7\,\partial q_8 = 0.0791(4)$ D. Zeeman splittings of ethylene in a magnetic field of approximately 2.5 kG were also observed. Since the infrared radiation was right-handed circularly polarized and the axial magnetic field was along the direction of the beam, only the $\Delta m = +1$ transitions were observed. The tensor components of the rotational g factors were determined to be $g_{aa} = -0.424(8)$, $g_{bb} = -0.123(8)$, and $g_{cc} = 0.037(6)$. A qualitative discussion on the relationship of the electronic structure of ethylene and the rotational g factors is given.

I. INTRODUCTION

Since molecules with a center of symmetry do not possess a permanent dipole moment, their Stark shift is caused only by the polarizabilities, i.e., the second order Stark effect between widely separated electronic and vibrational states. The shift is then very small, and a high resolution spectroscopic technique is needed for its observation. Stark shift measurements for such molecules have been so far limited to homonuclear diatomic molecules, such as H_2, D_2, O_2, I_2, and the linear molecule CO_2. MacAdam and Ramsey[1] studied the Stark effects in H_2 and D_2 using a molecular beam magnetic resonance technique. Gustafson and Gordy[2] studied O_2 using the magnetically induced microwave transitions. I_2 was studied by Callahan, Yokozeki, and Muenter[3] using laser-induced fluorescence spectroscopy. The Stark effect of CO_2 was recently observed by Gough, Orr, and Scoles[4] using optothermal infrared spectroscopy and a supersonic beam. In this paper we report the first observation of the Stark effect in a nonlinear molecule with a center of symmetry, ethylene. We observed sizable Stark shifts which are much larger than expected simply from the polarizability anisotropy. This is due to the second order Stark shift caused by the near degeneracy of the ν_7 and the ν_8 vibrational states.

We also observed the Zeeman effect in ethylene due to its rotational magnetic moment. All studies of the diamagnetic Zeeman effect for nonpolar molecules have been carried out using molecular beam technique. Ramsey and coworkers[5] made systematic measurements for a number of molecules with a center of symmetry, such as H_2, D_2, N_2, F_2, C_2H_2, etc. In the present paper, we determine the rotational g factors of ethylene for both the ν_7 state and the ground state. This provides information on the magnetic properties of ethylene. Such information for ethylene was previously available only indirectly through the study of Zeeman effect in the van der Waals complex of ethylene reported by Kukolich, Aldrich, Read, and Campbell.[6]

Both the Stark and Zeeman splittings in ethylene are in the range of a few MHz. In order to resolve such a small splitting in the infrared region, sub-Doppler spectroscopy using a tunable infrared source with high spectral purity is necessary. Microwave modulated sidebands generated on CO_2 laser radiation provides such an infrared source.

II. EXPERIMENTAL

The apparatus used for generating microwave sidebands on CO_2 laser radiation is identical to the one previously described.[7] Stabilized CO_2 laser radiation (ν_l) of 3 W and microwave radiation (ν_m, 12–18 GHz) of 20 W are combined in a CdTe crystal to generate sidebands ($\nu_l \pm \nu_m$) with power of $\sim$2 mW. The tunability of the resulting sidebands is 6 GHz on either side of each CO_2 laser line. The $10P(12)$ and the $10P(14)$ CO_2 laser lines used for the measurements are stabilized using SF_6 $R(66)$ $A_1^0F_1^0F_2^0A_2^0$ and SF_6 $R(28)$ A_2^0 absorption dips,[8] respectively. The spectral purity of the sidebands is $\sim$10 kHz, and the long term stability is within 30 kHz for several hours. Since a Fresnel rhomb is in the optical path, the infrared sideband radiation in the sample cell is right-handed circularly polarized (see Fig. 1).

Stark effects were measured using a dry ice cooled 45 cm sample cell which contained a pair of 40×5 cm^2 stainless steel Stark plates separated by 3.23 mm. Since the sample

 0021-9606/88/095282-09$02.10

cell was 5 cm longer than the Stark plates, the molecules in the field-free region gave a normal Lamb dip which appeared simultaneously with the Stark Lamb dips. This field-free signal provided a convenient frequency reference for measuring the Stark shifts. The dc voltage applied between the Stark plates was measured by a digital multimeter following a voltage divider. An electric field of up to 50 kV/cm was applied. The electric field was perpendicular to the direction of propagation of the circularly polarized infrared sideband radiation, and we observed transitions with the selection rules $\Delta m = 0, \pm 1$.

In the Zeeman measurement, a 85 cm long water cooled sample cell was placed inside a 50 cm long magnetic solenoid. Since the sample cell was longer than the solenoid, again a field-free signal coexisted with the Zeeman spectrum. This field-free signal was used as a frequency reference. The applied magnetic field was up to 2.5 kG and was calibrated using a Gaussmeter. The magnetic field was along the direction of propagation of the right-handed circularly polarized infrared radiation; as a result, we observed only the $\Delta m = +1$ transitions. The Zeeman pattern was thus much simpler than the Stark pattern which contained all the allowed transitions ($\Delta m = 0, \pm 1$).

III. THEORY

A. Stark effect

The Hamiltonian for a molecule in an electric field ϵ is

$$\hat{H} = \hat{H}_0 + \hat{H}_s, \quad \hat{H}_s = -\hat{\mu}\cdot\epsilon, \tag{1}$$

where $\hat{H}_0$ is the Hamiltonian of a field-free molecule and $\hat{\mu}$ is the electric dipole moment operator of the molecule. Since the energy separations for electronic states (ΔE_e), vibrational states (ΔE_v), and rotational levels (ΔE_r) are different by orders of magnitude ($\Delta E_e : \Delta E_v : \Delta E_r \sim 1 : \kappa^2 : \kappa^4$, where $\kappa \sim 0.1$ is the Born–Oppenheimer constant), we can apply the Van Vleck perturbation method[9] to calculate the Stark energy. The first and the second order electronic averages give

$$\langle \hat{H}_s \rangle = -\langle 0|\hat{\mu}|0\rangle\cdot\epsilon + \epsilon^+\cdot \sum_{n\neq 0} \frac{|\langle 0|\hat{\mu}|n\rangle|^2}{E_0 - E_n}\cdot\epsilon, \tag{2}$$

where E_0 and E_n are the energies for the ground and excited electronic states, respectively. Equation (2) can be rewritten using the usual notation as

$$\langle \hat{H}_s \rangle = -\mu\cdot\epsilon - \tfrac{1}{2}\epsilon^+\cdot\alpha_e\cdot\epsilon, \tag{3}$$

where μ is the "permanent" dipole moment and

$$\alpha_e = -2 \sum_{n\neq 0} \frac{|\langle 0|\hat{\mu}|n\rangle|^2}{E_0 - E_n} \tag{4}$$

is the electronic polarizability tensor. In order to calculate the vibrational average of the first term of Eq. (3), we expand the dipole moment μ into a power series of dimensionless normal coordinates q_s as

$$\mu = \mu_e + \sum_s \left(\frac{\partial \mu}{\partial q_s}\right)_e q_s + \frac{1}{2}\sum_{s,t}\left(\frac{\partial^2 \mu}{\partial q_s \partial q_t}\right)_e q_s q_t + \cdots. \tag{5}$$

Because of the presence of the center of symmetry in ethylene, $\mu_e = 0$. The first order average of the third term vanishes for the same reason. Thus the second order vibrational average of the Stark energy is

$$\langle \hat{H}_s \rangle = -\tfrac{1}{2}\epsilon^+\cdot(\alpha_e + \alpha_v)\cdot\epsilon, \tag{6}$$

where

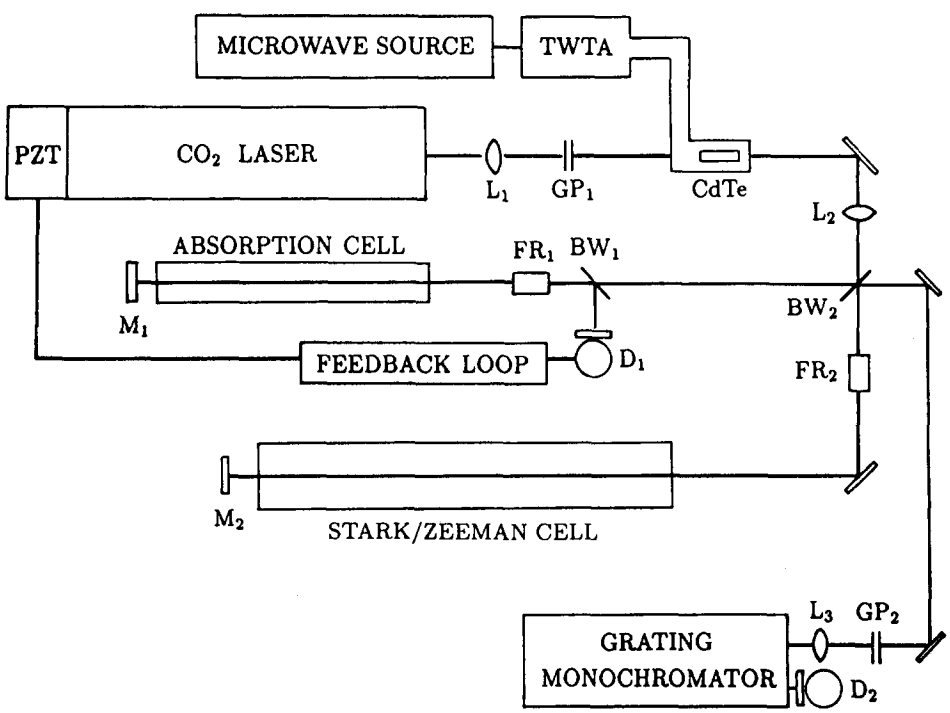

FIG. 1. Experimental setup. BW_1, BW_2: Brewster-angle windows; D_1, D_2:HgCdTe detectors; FR_1, FR_2: Fresnel rhobms; GP_1, GP_2: grid polarizer; L_1, L_2, L_3: ZnSe lenses; M_1, M_2: concave reflection mirrors; PZT: piezoelectric translator; TWTA: traveling wave tube amplifier.

$$\alpha_v = -2\sum_{l\neq k}\sum_s \frac{|\langle k|q_s|l\rangle|^2}{E_k - E_l}\left(\frac{\partial\mu}{\partial q_s}\right)_e^2 \tag{7}$$

is the vibrational polarizability for the $|k\rangle$ vibrational state. There is one term in Eq. (5) which needs special treatment. This is the term $\frac{1}{2}(\partial^2\mu_a/\partial q_7\,\partial q_8)_e q_7 q_8$ which connects two vibrational states with a small separation ($\nu_7 - \nu_8 = 8.91$ cm^{-1}) comparable to the rotational energy level spacing. We have to treat this term separately. We thus have the total Stark Hamiltonian

$$H_s = -\frac{1}{2}\epsilon^+\cdot\alpha\cdot\epsilon - \frac{1}{2}\frac{\partial^2\mu_a}{\partial q_7\,\partial q_8}\cdot\epsilon q_7 q_8, \tag{8}$$

where $\alpha \equiv \alpha_e + \alpha_v$. Both α_e and α_v are diagonal from the three C_2 axes of symmetry. We now calculate the rotational average of the first term of Eq. (8)

$$\begin{aligned} H' &= -\tfrac{1}{2}\epsilon^+\cdot\alpha\cdot\epsilon, \\ &= -\tfrac{1}{2}\epsilon^2(\alpha_{aa}\Phi_{Za}^2 + \alpha_{bb}\Phi_{Zb}^2 + \alpha_{cc}\Phi_{Zc}^2), \end{aligned} \tag{9}$$

where $\alpha_{\xi\xi}$ ($\xi = a,b,c$) are the diagonal components of the polarizability tensor along the molecule-fixed a,b,c axes and $\Phi_{Z\xi}$ are the direction cosines between the ξ-axis and the space-fixed Z axis which is taken to be along the direction of the electric field. Equation (9) can be averaged and rearranged as

$$\begin{aligned} \langle H'\rangle = -\frac{1}{2}\epsilon^2\Bigg\{&\frac{\alpha_{bb}+\alpha_{cc}}{2} + (\alpha_{aa} - \frac{\alpha_{bb}+\alpha_{cc}}{2})\langle\Phi_{Za}^2\rangle \\ &+ \frac{\alpha_{bb}-\alpha_{cc}}{2}(\langle\Phi_{Zb}^2\rangle - \langle\Phi_{Zc}^2\rangle)\Bigg\} \end{aligned} \tag{10}$$

and the value of the square of direction cosines averaged by asymmetric rotor wave function $\langle\Phi_{Z\xi}^2\rangle$ can be calculated for individual levels by expanding the rotational wave function into a series of symmetric rotor wave functions and using the usual direction cosine matrix elements.

The second term in Eq. (8) can be written as

$$H'' = -\delta\mu_a\Phi_{Za}\epsilon q_7 q_8, \tag{11}$$

where $\delta\mu_a = \frac{1}{2}(\partial^2\mu_a/\partial q_7\,\partial q_8)$; from the symmetries of $q_7(B_{1u})$ and $q_8(B_{2g})$ (Fig. 2), only $\delta\mu_a(B_{3u})$ is allowed. The term H'' mixes the state $|1\rangle = |v_7 = 1, v_8 = 0, J_{k_a k_c}\rangle$ with other states $|n\rangle = |v_7 = 0, v_8 = 1, J'_{k_a k_c \pm 1}\rangle$.

The Stark energy shift due to these mixings is then

$$\Delta\nu = \frac{1}{h}\sum_n \frac{|\langle 1|H''|n\rangle|^2}{E_1 - E_n}. \tag{12}$$

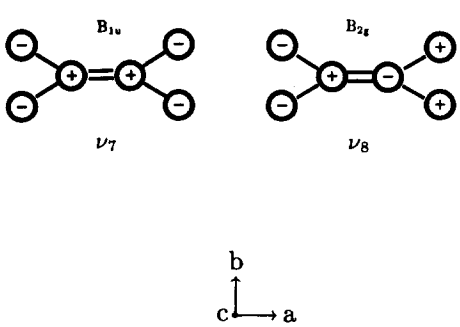

FIG. 2. The ν_7 and the ν_8 vibrational modes of ethylene with symmetries B_{1u} and B_{2g}, respectively, in the D_{2h} point group.

B. Zeeman effect

The Zeeman effect Hamiltonian describing the interaction of the rotational magnetic moment (μ_m) of a molecule and an external magnetic field (B), which is along the direction of the space-fixed Z axis, can be expressed as

$$\begin{aligned} H &= -\mu_m\cdot\mathbf{B}, \\ &= -B\sum_\xi \mu_\xi\,\Phi_{Z\xi}, \\ &= -\mu_n B\sum_{\xi,\eta} g\xi\eta\, J_\eta\,\Phi_{Z\xi}, \end{aligned} \tag{13}$$

where μ_n is the nuclear magneton, $g_{\xi\eta}$ ($\xi,\eta = a,b,c$) are the components of the rotational g tensor along the molecule-fixed axes, and J_η are the components of the dimensionless rotational angular momentum. Choosing the molecule-fixed axes along the axis of C_2 symmetry, Eq. (13) is diagonalized to be

$$H = -\mu_n B\sum_\xi g_{\xi\xi}J_\xi\Phi_{Z\xi}. \tag{14}$$

Since J_ξ is diagonal with respect to the total angular momentum quantum number J and we are calculating the diagonal matrix element of H, only the diagonal matrix element of $\Phi_{Z\xi}$ is relevant. In such a case we can replace $\Phi_{Z\xi}$ with $(J_Z J_\xi/J^2) = [m/\sqrt{J(J+1)}]\,[J_\xi/\sqrt{J(J+1)}]$, where m is the magnetic quantum number. Equation (14) can then be written as

$$H = -\mu_n B\frac{m}{J(J+1)}\sum_\xi g_{\xi\xi}J_\xi^2. \tag{15}$$

The splitting of a rotational energy level due to Zeeman effect can thus be expressed as

$$\begin{aligned} \Delta W = \langle H\rangle = -\mu_n B\frac{m}{J(J+1)}&(g_{aa}\langle J_a^2\rangle + g_{bb}\langle J_b^2\rangle \\ &+ g_{cc}\langle J_c^2\rangle), \end{aligned} \tag{16}$$

where $\langle J_\xi^2\rangle$ ($\xi = a,b,c$) are the averages of J_ξ^2 with the asymmetric rotor wave function. They can be calculated from the asymmetric rotor energy experssion for a prolate rotor[10]:

$$\frac{W_r}{h} = \frac{1}{2}(B+C)J(J+1) + \left[A - \frac{1}{2}(B+C)\right]\omega(b), \tag{17}$$

where $b = (C-B)/(2A-B-C)$ is the asymmetry parameter, as

$$\begin{aligned} \langle J_a^2\rangle &= \frac{\partial W_r}{\partial A} = \omega(b) - b\frac{d\omega(b)}{db}, \\ \langle J_b^2\rangle &= \frac{\partial W_r}{\partial B} = \frac{1}{2}\{J(J+1) - \omega(b) + (b-1)\frac{d\omega(b)}{db}\}, \\ \langle J_c^2\rangle &= \frac{\partial W_r}{\partial C} = \frac{1}{2}\{J(J+1) - \omega(b) + (b+1)\frac{d\omega(b)}{db}\}. \end{aligned} \tag{18}$$

Thus we have from Eqs. (16) and (18),

$$\Delta W = -\mu_n g_J m B, \tag{19}$$

where

$$g_J = \frac{1}{J(J+1)}\left\{\left[\omega(b) - b\frac{d\omega(b)}{db}\right]g_{aa} + \frac{1}{2}\left[J(J+1) - \omega(b) + (b-1)\frac{d\omega(b)}{db}\right]g_{bb} + \frac{1}{2}\left[J(J+1) - \omega(b) + (b+1)\frac{d\omega(b)}{db}\right]g_{cc}\right\}.$$

The diagonal elements of the g tensor are given by[11]

$$g_{\xi\xi} = \frac{2m_p}{I_{\xi\xi}}\left\{\sum_i \frac{Z_i}{2}(\eta_i^2 + \zeta_i^2) + \frac{1}{m_e}\sum_{n\neq 0}\frac{|\langle 0|\hat{L}_\xi|n\rangle|^2}{E_0 - E_n}\right\}, \tag{20}$$

where m_p is the mass of proton, and $I_{\xi\xi}$ is the moment of inertia along the ξ axis. The first term in Eq. (20) corresponds to the positive magnetic moment produced by the rotation of nuclei; ξ_i, η_i, and ζ_i are the positions of ith nucleus with electronic charge $Z_i e$. The second term in Eq. (20) corresponds to the negative magnetic moment due to the partial excitation of excited electronic state by rotation of the molecule, where the summation is over all possible electronic excited states and $\hat{L}_\xi$ is the operator of the electronic orbital angular momentum along the ξ axis.

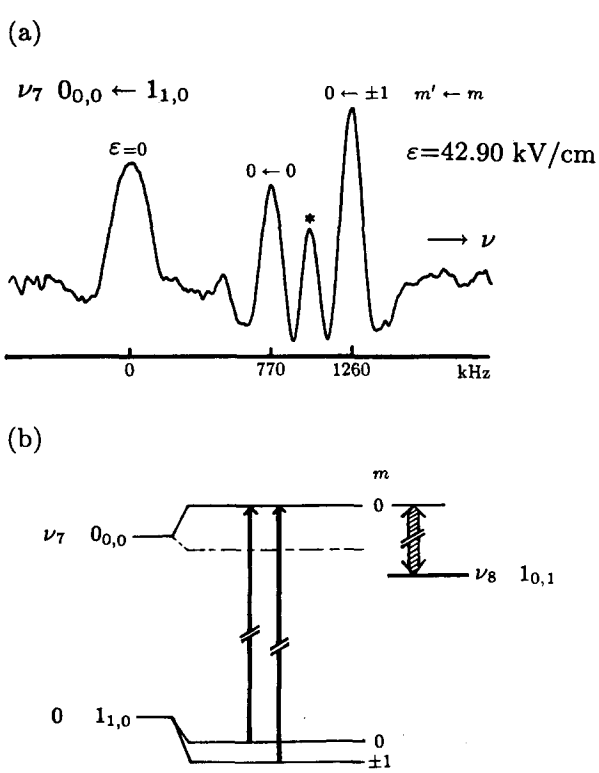

FIG. 3. (a) Observed inverse Lamb-dip Stark spectrum of the rovibrational transition of ν_7 $0_{0,0} \leftarrow 1_{1,0}$ of ethylene in an electric field of 42.90 kV/cm. The normal dip (at 0 kHz) caused by the field-free molecules ($\epsilon = 0$) is taken as a frequency reference in the measurement of Stark shifts. The two normal dips corresponding to the transitions of $0 \leftarrow 0$ and $0 \leftarrow \pm 1$ ($m' \leftarrow m$, m', and m are magnetic quantum numbers of ν_7 excited and the ground states, respectively) with their crossover dip marked by an asterisk are observed. The upper microwave sideband of CO_2 10 $P(22)$ laser line with ν_m ~15 630 MHz was used. Modulation: FM at 100 kHz, time constant 4 s. Sample pressure: 2 mTorr. (b) The diagram of the ν_7 $0_{0,0}$ state perturbed by the ν_8 $1_{0,1}$ state due to a second order Stark effect in ethylene. The broken line represents the energy level expected from the polarizability of the ν_7 state alone.

IV. OBSERVED RESULTS

A. Stark effect

The observed Stark pattern of the rovibrational transition ν_7 $0_{0,0} \leftarrow 1_{1,0}$ of ethylene in an electric field of 42.90 kV/cm is shown in Fig. 3(a). The two sharp features at 770 and 1260 kHz are normal saturation dips corresponding to the $m = 0 \leftarrow 0$ and $0 \leftarrow \pm 1$ transitions. The center dip between them marked with an asterisk is the crossover dip caused by these two transitions which have a common level in the ν_7 excited state [see Fig. 3(b)]. The broad feature at 0 kHz is the transition caused by the field-free ($\epsilon = 0$) molecules which are outside the Stark plates. This signal provides a convenient frequency reference for the measurement of Stark shifts. The larger width of the $\epsilon = 0$ signal is mostly due to power broadening but may also be partly due to stray electric field in the field-free region.

The observed Stark shift of ethylene was much greater than what we anticipated simply from estimated polarizability. This is because of the extra Stark shift in the ν_7 excited state due to its accidental degeneracy with the ν_8 state. This situation is shown in Fig. 3(b). The ground state $1_{1,0}$ lowers its energy when the Stark field is applied due to polarizability. The same effect lowers the $0_{0,0}$ level of the ν_7 state (shown by broken lines) but this lowering of the level is overcompensated by the raising of the level due to the second order Stark effect by near degenerate ν_8 $1_{0,1}$ level.

The observed Stark pattern of the ν_7 $1_{1,0} \leftarrow 2_{2,0}$ transition at $\epsilon = 40.35$ kV/cm is shown in Fig. 4. Here the three

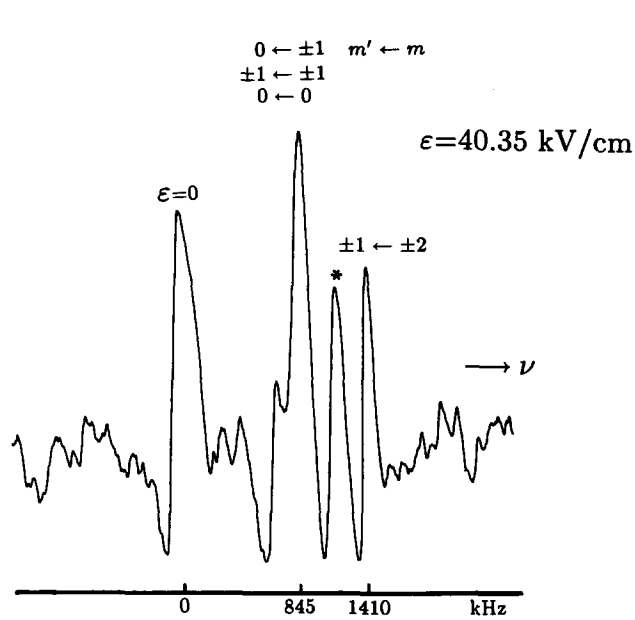

FIG. 4. Observed inverse Lamb-dip Stark spectrum of ν_7 $1_{1,0} \leftarrow 2_{2,0}$ transition of ethylene in an electric field of 40.35 kV/cm. The strong center feature corresponds to the three overlapped transitions. The $\pm 1 \leftarrow \pm 2$ normal dip with its crossover dip correlating to the $\pm 1 \leftarrow \pm 1$ transition are well resolved. The upper microwave sideband of CO_2 10 $P(32)$ laser line with ν_m ~16 140 MHz was used. Modulation: FM at 85 kHz, time constant 4 s. Sample pressure: 3 mTorr.

transitions $m = 0 \leftarrow \pm 1$, $\pm 1 \leftarrow \pm 1$, and $0 \leftarrow 0$ were not resolved and appeared as one strong Lamb dip. The $m = \pm 1 \leftarrow \pm 2$ dip is well separated and a crossover dip is produced between them. The Stark shift is much enhanced due to the shift of ν_7 $1_{1,0}$ level towards higher energy caused by the nearby low-lying levels of ν_8 $1_{1,1}$ and ν_8 $2_{1,1}$.

A more complicated observed Stark pattern for $\nu_7 5_{1,5} \leftarrow 5_{0,5}$ is shown in Fig. 5. Two traces of the patterns are shown to demonstrate the frequency stability of our infrared sideband source which is $\leqslant 30$ kHz for several hours. Many measurements were made for each transition at different electric fields. The results are summarized in Table I.

B. Zeeman effect

The observed Zeeman patterns are much simpler than the Stark patterns partly because of the linear dependence of the Zeeman shift on the field but also because of the $\Delta m = +1$ (only) selection rule due to the circular polarization of the radiation and the collinear magnetic field and beam direction. The selection rule drops off half of the Zeeman pattern and eliminates the possibility of crossover dips. The simple Zeeman pattern for the ν_7 $0_{0,0} \leftarrow 1_{1,0}$ and ν_7 $1_{1,0} \leftarrow 2_{2,0}$ transitions are shown in Fig. 6. Here the patterns are composed of only one Zeeman shifted line and the field-free line. Somewhat more complicated cases of the ν_7 $2_{1,1} \leftarrow 2_{2,1}$ and ν_7 $3_{0,3} \leftarrow 2_{1,1}$ transitions are given in Fig. 7. The relative intensities of different components of Zeeman pattern as well as those of Stark pattern are not equal to the values calculated from a simple intensity formula because of the nonlinearity of saturation spectroscopy.

The measurements of Zeeman shifts were done for each transition for various magnetic fields. The observed slopes of the Zeeman shift in kHz/G are listed in Table II.

V. ANALYSIS

A. Stark effect

The average of the polarizability Hamiltonian given in Eq. (10) are calculated for each rotational level. In the calculation we used a linear combination of the symmetric rotor wave functions $\psi_{\pm} = [\psi(J,k) \pm \psi(J,-k)]/\sqrt{2}$. We find that, since the asymmetry parameter is very small ($b = -0.021$) for ethylene, the asymmetric rotor correction is negligible for low J and K rotational levels. Using this approximation the polarizability shifts are calculated using the averages of $\Phi^2_{Z\xi}$ listed in Table III.

The second order Stark shift caused by the off-diagonal Hamiltonian H'' of Eq. (8) are calculated from the off-diagonal matrix element and the energy difference ΔE between the perturbed states given in Table III. The latter were calculated using the molecular constants of the ν_7 state and of the ν_8 state kindly provided to us by Fayt.[12] The second order Stark shift is calculated by Eq. (12). Thus for the many observed second order Stark shifts given in Table I, we have a linear simultaneous equation with unknown constants $\alpha_{aa} - \frac{1}{2}(\alpha_{bb} + \alpha_{cc})$, $\alpha_{bb} - \alpha_{cc}$ each for the ground and the ν_7 states, the difference $(\alpha_{bb} + \alpha_{cc})_{\nu_7} - (\alpha_{bb} + \alpha_{cc})_{gr}$ and $\delta\mu_a$. The six constants have been determined by a least-squares fitting of the observed Stark shifts. The determined constants are shown in Table IV. We can determine individual values of α_{aa}, α_{bb}, and α_{cc} combining these results with $\bar{\alpha} = \frac{1}{3}(\alpha_{aa} + \alpha_{bb} + \alpha_{cc}) = 4.254$ Å^3 obtained by Bose and Cole.[13,14] They are shown in Table V. The optical polarizability components of ethylene determined from the relative intensities of Raman effect by Hills and Jones[15] are also listed. The similarity of this result to ours will be discussed later.

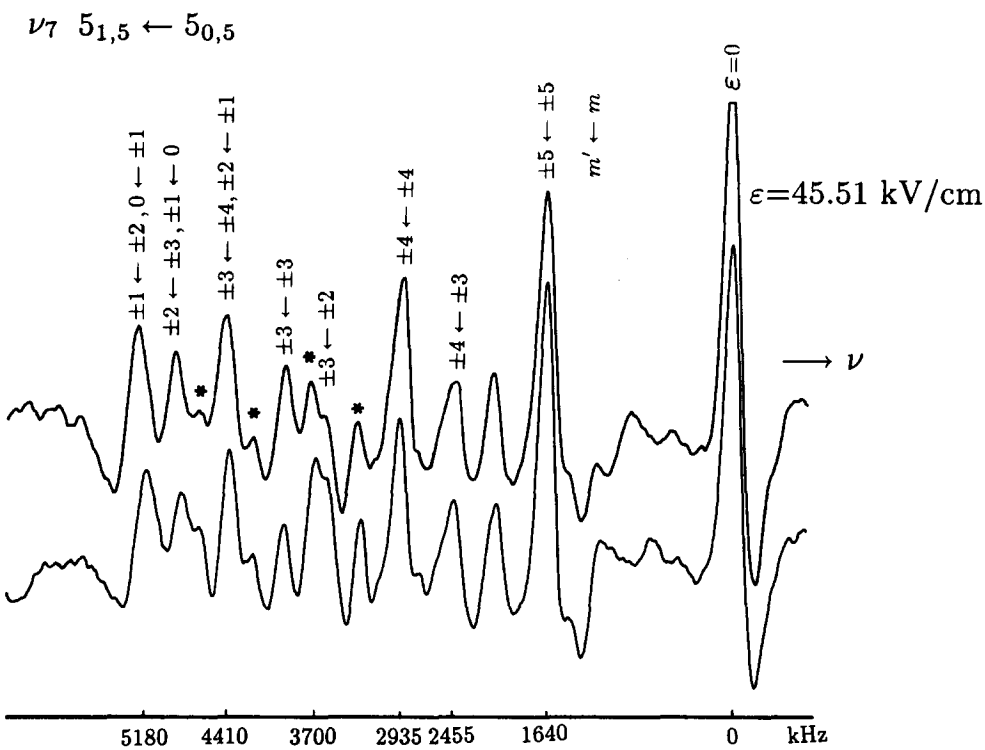

FIG. 5. Observed inverse Lamb-dip Stark spectrum of ν_7 $5_{1,5} \leftarrow 5_{0,5}$ transition of ethylene in an electric field of 45.51 kV/cm. The normal dips have been assigned $m' \leftarrow m$ values; the crossover dips are shown by *. The reproducibility of the Stark patterns indicates the stability of our laser. The upper microwave sideband of CO_2 10 $P(12)$ laser line with $\nu_m \sim 16\,375$ MHz was used. Modulation: FM at 100 kHz, time constant 4 s. Sample pressure: 2 mTorr.

TABLE I. The observed Stark shifts $\Delta\nu/\epsilon^2$ of ethylene [in kHz/(kV/cm)^2].

Transition	$m' \leftarrow m$	Intensity[a]	Polarizability: ν_7	Polarizability: ground	Second order dipole	Total	Observed
$0_{0,0} \leftarrow 1_{1,0}$	$0 \leftarrow 0$	1/3	−0.510	−0.330	0.621	0.441	0.422 ± 0.025
	$0 \leftarrow \pm 1$	1/3	−0.510	−0.646	0.621	0.757	0.679 ± 0.025
$1_{1,0} \leftarrow 2_{2,0}$	$\pm 1 \leftarrow 0$	1/20	−0.628	−0.228	0.720	0.320	
	$0 \leftarrow 0$	1/5	−0.336	−0.228	0.490	0.382	
	$\pm 1 \leftarrow \pm 1$	3/10	−0.628	−0.380	0.720	0.471	0.519 ± 0.025[b]
	$0 \leftarrow \pm 1$	3/20	−0.336	−0.380	0.490	0.534	
	$\pm 1 \leftarrow \pm 2$	3/10	−0.628	−0.835	0.720	0.927	0.866 ± 0.027
$2_{1,1} \leftarrow 2_{2,1}$	$\pm 1 \leftarrow 0$	1/12	−0.600	−0.228	0.960	0.587	
	$\pm 2 \leftarrow \pm 1$	1/18	−0.392	−0.380	0.632	0.621	
	$\pm 1 \leftarrow \pm 1$	1/18	−0.600	−0.380	0.960	0.739	
	$0 \leftarrow \pm 1$	1/12	−0.670	−0.380	1.069	0.779	
	$\pm 2 \leftarrow \pm 2$	2/9	−0.392	−0.835	0.632	1.076	1.031 ± 0.020[b]
	$\pm 1 \leftarrow \pm 2$	1/18	−0.600	−0.835	0.960	1.195	
$3_{0,3} \leftarrow 2_{1,1}$	$\pm 3 \leftarrow \pm 2$	1/7	−0.179	−0.390	0.878	1.089	1.082 ± 0.014
	$\pm 2 \leftarrow \pm 2$	2/21	−0.510	−0.390	1.636	1.516	1.549 ± 0.027
	$\pm 2 \leftarrow \pm 1$	2/21	−0.510	−0.616	1.636	1.742	1.776 ± 0.022
	$\pm 1 \leftarrow \pm 2$	1/105	−0.709	−0.390	2.091	1.772	
	$\pm 1 \leftarrow \pm 1$	16/105	−0.709	−0.616	2.091	1.998	
	$\pm 1 \leftarrow 0$	2/35	−0.709	−0.691	2.091	2.073	2.065 ± 0.014[b]
	$0 \leftarrow \pm 1$	1/35	−0.776	−0.616	2.243	2.083	
	$0 \leftarrow 0$	3/35	−0.776	−0.691	2.243	2.159	
$5_{1,5} \leftarrow 5_{0,5}$	$\pm 5 \leftarrow \pm 4$	1/12	−0.138	−0.368	−0.780	−0.551	
	$\pm 5 \leftarrow \pm 5$	5/6	−0.138	−0.123	−0.780	−0.796	-0.794 ± 0.013
	$\pm 4 \leftarrow \pm 3$	3/20	−0.349	−0.559	−1.418	−1.209	-1.177 ± 0.024
	$\pm 4 \leftarrow \pm 4$	8/15	−0.349	−0.368	−1.418	−1.400	-1.414 ± 0.014
	$\pm 4 \leftarrow \pm 5$	1/12	−0.349	−0.123	−1.418	−1.645	
	$\pm 3 \leftarrow \pm 2$	1/5	−0.513	−0.695	−1.915	−1.733	-1.713 ± 0.013
	$\pm 3 \leftarrow \pm 3$	3/10	−0.513	−0.559	−1.915	−1.869	-1.883 ± 0.018
	$\pm 3 \leftarrow \pm 4$	3/20	−0.513	−0.368	−1.915	−2.060	
	$\pm 2 \leftarrow \pm 1$	7/30	−0.630	−0.777	−2.269	−2.123	-2.124 ± 0.033[b]
	$\pm 2 \leftarrow \pm 2$	2/15	−0.630	−0.695	−2.269	−2.204	
	$\pm 2 \leftarrow \pm 3$	1/5	−0.630	−0.559	−2.269	−2.341	-2.341 ± 0.018[b]
	$\pm 1 \leftarrow 0$	1/4	−0.701	−0.804	−2.482	−2.378	
	$\pm 1 \leftarrow \pm 1$	1/30	−0.701	−0.777	−2.482	−2.406	
	$\pm 1 \leftarrow \pm 2$	7/30	−0.701	−0.695	−2.482	−2.488	-2.500 ± 0.020[b]
	$0 \leftarrow \pm 1$	1/4	−0.724	−0.777	−2.553	−2.500	

[a] Square of the matrix element of direction cosine.
[b] Unresolved signals.

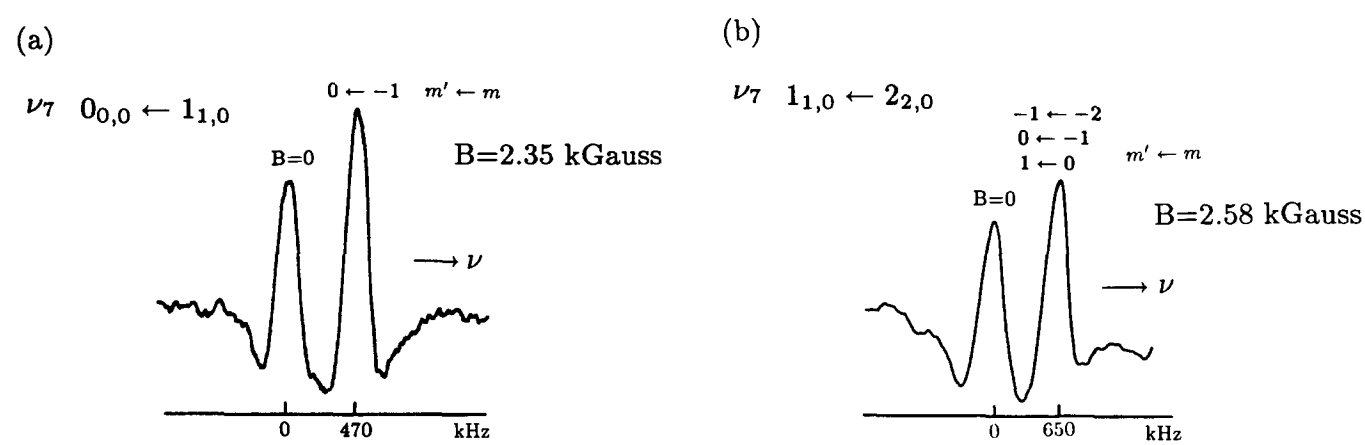

FIG. 6. (a) Observed inverse Lamb-dip Zeeman spectrum of ν_7 $0_{0,0} \leftarrow 1_{1,0}$ transition of ethylene in a magnetic field of 2.35 kG. The upper microwave sideband of CO_2 10 $P(22)$ laser line with $\nu_m \sim 15\,630$ MHz was used. Modulation: FM at 110 kHz, time constant 1.25 s. Sample pressure: 6 mTorr. (b) Observed invese Lamb-dip Zeeman spectrum of ν_7 $1_{1,0} \leftarrow 2_{2,0}$ transition of ethylene in a magnetic field of 2.58 kG. The upper microwave sideband of CO_2 10 $P(32)$ laser line with $\nu_m \sim 16\,140$ MHz was used. Modulation: FM at 100 kHz, time constant 4 s. Sample pressure: 8 mTorr.

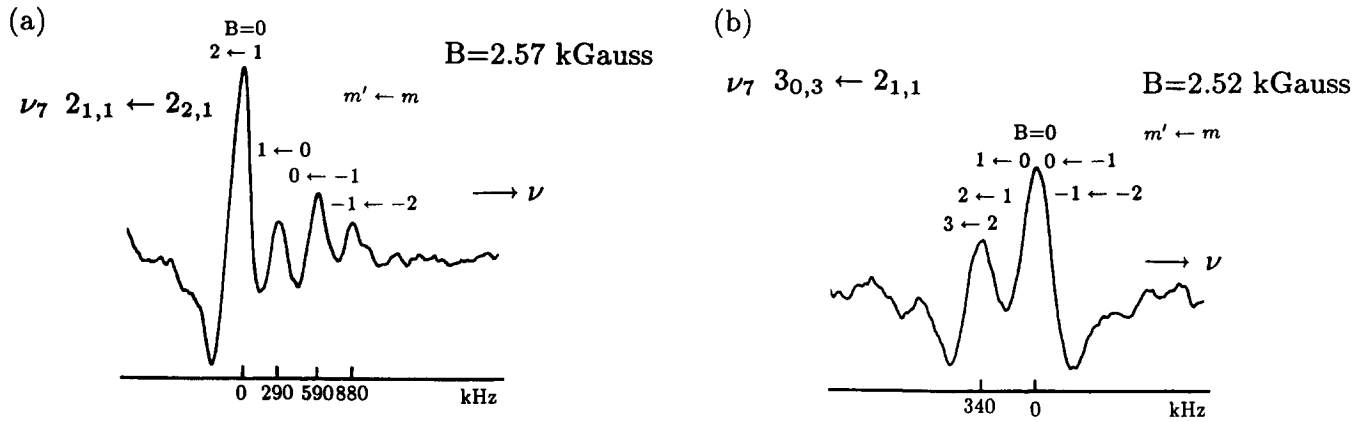

FIG. 7. (a) Observed inverse Lamb-dip Zeeman spectrum of ν_7 $2_{1,1} \leftarrow 2_{2,1}$ transition of ethylene in a magnetic field of 2.57 kG. The upper microwave sideband of CO_2 10 $P(28)$ laser line with $\nu_m \sim 15\,460$ MHz was used. Modulation: FM at 100 kHz, time constant 4 s. Sample pressure: 6 mTorr. (b) Observed inverse Lamb-dip Zeeman spectrum of ν_7 $3_{0,3} \leftarrow 2_{1,1}$ transition of ethylene in a magnetic field of 2.52 kG. The upper microwave sideband of CO_2 10 $P(14)$ laser line with $\nu_m \sim 15\,530$ MHz was used. Modulation: 115 kHz, time constant 4 s. Sample pressure: 9 mTorr.

TABLE II. The observed Zeeman shift $\Delta\nu/B$ of ethylene due to three components of the g tensor (in kHz/G).

Transition	$m' \leftarrow m$	Intensity[a]	a	b	c	Total	Observed
$0_{0,0} \leftarrow 1_{1,0}$	$0 \leftarrow -1$	1/6	0.162	0.047	0.000	0.209	0.200 ± 0.011
$1_{1,0} \leftarrow 2_{2,0}$	$1 \leftarrow 0$	1/40	0.162	0.047	0.000	0.209	
	$0 \leftarrow -1$	3/40	0.216	0.017	−0.004	0.228	
	$-1 \leftarrow -2$	3/20	0.269	−0.014	−0.009	0.247	0.252 ± 0.008[b]
$2_{1,1} \leftarrow 2_{2,1}$	$2 \leftarrow 1$	1/36	−0.108	0.109	−0.005	−0.003	
	$1 \leftarrow 0$	1/24	0.054	0.063	−0.005	0.112	0.113 ± 0.006
	$0 \leftarrow -1$	1/24	0.216	0.016	−0.005	0.227	0.223 ± 0.008
	$-1 \leftarrow -2$	1/36	0.377	−0.031	−0.005	0.342	0.332 ± 0.008
$3_{0,3} \leftarrow 2_{1,1}$	$3 \leftarrow 2$	1/14	−0.107	0.008	−0.035	−0.134	-0.135 ± 0.005[b]
	$2 \leftarrow 1$	1/21	−0.054	0.026	−0.025	−0.052	
	$1 \leftarrow 0$	1/35	0.000	0.044	−0.015	0.030	
	$0 \leftarrow -1$	1/70	0.054	0.063	−0.005	0.112	
	$-1 \leftarrow -2$	1/210	0.108	0.081	0.005	0.194	

[a] Square of the matrix element of direction cosine.
[b] Unresolved signals.

TABLE III. Calculated values of the squares of the direction cosines for rotational levels, and the coupling between the ν_7 and the ν_8 rotation–vibrational levels of ethylene using symmetric rotor approximation (m: magnetic quantum number).

	Φ^2_{Za}	Φ^2_{Zb}	Φ^2_{Zc}
$0_{0,0}$	1/3	1/3	1/3
$1_{1,0}$	$(1+m^2)/5$	$(12-3m^2)/20$	$(4-m^2)/20$
$2_{2,0}, 2_{2,1}$	$(3+2m^2)/21$	$(9-m^2)/21$	$(9-m^2)/21$
$2_{1,1}$	$(9-m^2)/21$	$(12+m^2)/28$	$(12+m^2)/84$
$3_{0,3}$	$(23-2m^2)/45$	$(11+m^2)/45$	$(11+m^2)/45$
$5_{1,5}$	$(95-3m^2)/195$	$(100+3m^2)/780$	$(100+3m^2)/260$
$5_{0,5}$	$(59-2m^2)/117$	$(29+m^2)/117$	$(29+m^2)/117$

ν_7	ν_8	$\Delta E = \nu_7 - \nu_8 (\mathrm{cm}^{-1})$	$H''/(\delta\mu_a\epsilon)$
$0_{0,0}$	$1_{0,1}$	7.085	$1/\sqrt{3}$
$1_{1,0}$	$1_{1,1}$	9.369	$m/2$
$1_{1,0}$	$2_{1,1}$	5.388	$\sqrt{4-m^2}/(2\sqrt{5})$
$2_{1,1}$	$1_{1,0}$	13.016	$\sqrt{4-m^2}/(2\sqrt{5})$
$2_{1,1}$	$2_{1,2}$	9.701	$m/6$
$2_{1,1}$	$3_{1,2}$	3.484	$2\sqrt{2}\sqrt{9-m^2}/(3\sqrt{35})$
$3_{0,3}$	$2_{0,2}$	14.363	$\sqrt{9-m^2}/\sqrt{35}$
$3_{0,3}$	$4_{0,4}$	1.671	$\sqrt{16-m^2}/\sqrt{63}$
$5_{1,5}$	$4_{1,4}$	17.902	$2\sqrt{2}\sqrt{25-m^2}/(5\sqrt{33})$
$5_{1,5}$	$5_{1,4}$	6.730	$m/30$
$5_{1,5}$	$6_{1,6}$	−1.183	$\sqrt{35}\sqrt{36-m^2}/(6\sqrt{143})$

TABLE IV. Electric properties of ethylene determined from the Stark effect measurements.

	ν_7 state	Ground state
$\alpha_{aa} - (\alpha_{bb} + \alpha_{cc}/2)$	1.78(11) Å^3	1.91(13) Å^3
$\alpha_{bb} - \alpha_{cc}$	0.15(14) Å^3	0.07(19) Å^3
$(\alpha_{bb} + \alpha_{cc})_{\nu_7} - (\alpha_{bb} + \alpha_{cc})_{gr}$	0.03(07) Å^3	
$(\partial^2\mu_a/\partial q_7\,\partial q_8)$	0.0791(4) D	

TABLE V. Electronic and vibrational polarizabilities of ethylene (unit: Å^3).

	This work						Reference 15	Reference 19
	Static polarizability						Optical polarizability	*ab initio* calculation
	ν_7 state			Ground state				
	Total	Vib.	Elect.	Total	Vib.	Elect.	Total	Total
α_{aa}	5.44	0.03	5.41	5.53	0.03	5.50	5.40	5.24
α_{bb}	3.74	0.01	3.73	3.65	0.01	3.64	3.86	3.47
α_{cc}	3.58	0.36	3.22	3.58	0.36	3.22	3.40	3.11

B. Zeeman effect

Zeeman shifts can be calculated from Eq. (19) in terms of the three diagonal components of the g tensor. The explicit expression for each rotational level is given in Table VI. The observed linear Zeeman shifts were least-squares fitted to these patterns to determine the three parameters g_{aa}, g_{bb}, and g_{cc}. Since we could not resolve further splitting of the Zeeman components due to different values of $g_{\xi\xi}$ between the ground and the excited states, we assumed them to be equal. The computer fitting gave the values of $g_{\xi\xi}$ shown in Table VII. The values of $g_{\xi\xi}$ of ethylene determined by Kukolich *et al.*[6] from the Zeeman effect of van der Waals HCl---C_2H_4 molecule are also listed in the table. The agreement between the two sets of values is reasonable although the present results are more accurate. Their values of g_{bb} and g_{cc} depend on the assumed angles between the plane of ethylene and the a axis. Equating our values and their values for various angles, we find that the agreement is best when the plane of ethylene is perpendicular to the a axis. The values of g factors for H_2CO determined by Hüttner, Lo, and Flygare[16] are also listed for comparison.

VI. DISCUSSION

A. Stark effect

As discussed earlier in Sec. III, the molecular polarizability is composed of two terms, i.e., the electronic polarizability α_e and the vibrational polarizability α_v. The latter can be calculated if transition dipole moments of all infrared active bands are known. Using Eq. (7) we obtain the vibrational polarizability for the ground state to be

$$(\alpha_v)_{\xi\xi} = \sum_s \frac{1}{h\nu_s}\left(\frac{\partial\mu_\xi}{\partial q_s}\right)_e^2. \tag{21}$$

Using the transition dipole moments of ethylene given by Golike *et al.*[17] and Jalsovszky *et al.*,[18] we obtain the values of the three diagonal components of the vibrational polarizability tensor as listed in Table V. The values of electronic polarizability which are calculated from the observed values, and the calculated *ab initio* values are also given in the table. It is noticed that the vibrational polarizability values are much smaller than those for the electronic polarizability. For vibrational excited states the vibrational polarizability remains the same to the first order of approximation, because of the cancellation of the effects from upper state and those from the lower state. Thus Eq. (21) holds for any vibrational state except for the accidental degeneracy such as that between ν_7 and ν_8 which we considered separately in this work.

The electronic polarizability components determined in the experiment are compared with the optical polarizability determined from the relative intensities of Raman spectral lines by Hills and Jones[15] in Table V. In principle the optical polarizability components should be larger than the static polarizability components because for the optical polarizability we have to replace $E_0 - E_n$ in Eq. (4) by $E_0 - E_n - \hbar\omega$ where ω is the frequency of the optical radiation. The close agreement between the static and optical polarizabilities may be due to the fact that $\hbar\omega$ for the optical experiment is much smaller than the excitation energies for electronic transitions with a large transition moment. The *ab initio* theoretical values given by Komornicki and McIver[19] are also listed in Table V.

The magnitude of $(\partial^2\mu_a/\partial q_7\,\partial q_8) = 0.0791(4)$ D is

TABLE VI. The g_J values of rotational levels.

Level	g_J
$0_{0,0}$	0
$1_{1,0}$	$1/2g_{aa} + 1/2g_{bb}$
$2_{2,0}$	$0.6664g_{aa} + 0.1777g_{bb} + 0.1559g_{cc}$
$2_{1,1}$	$1/6g_{aa} + 2/3g_{bb} + 1/6g_{cc}$
$2_{2,1}$	$2/3g_{aa} + 1/6g_{bb} + 1/6g_{cc}$
$3_{0,3}$	$0.0005g_{aa} + 0.4737g_{bb} + 0.5258g_{cc}$

TABLE VII. Magnetic properties of ethylene.

	C_2H_4		H_2CO
	This work[a]	Ref. 6[b]	Ref. 16[b]
$(g_{aa})_{v_7} = (g_{aa})_{gr}$	−0.424(8)	−0.45(2)	−2.899(2)
$(g_{bb})_{v_7} = (g_{bb})_{gr}$	−0.123(8)	−0.19[c]	−0.2256(8)
$(g_{cc})_{v_7} = (g_{cc})_{gr}$	0.037(6)	0.10[c]	−0.1004(7)

[a] Rigorously speaking, these values should be represented as $\frac{1}{2}[(g_{\xi\xi})_{v_7} + (g_{\xi\xi})_{gr}]$ $(\xi = a,b,c)$. However, since the change of electronic distribution due to excitation of vibration is small, the assumption of $(g_{\xi\xi})_{v_7} = (g_{\xi\xi})_{gr}$ will be a good approximation. For example, the difference of electric dipole moments between vibrationally excited states and the ground state of simple polyatomic molecules is typically a few percent.

[b] At ground state.

[c] These values depend on the assumed vibrational amplitude for oscillation in the angle θ between the c axis of ethylene and the a axis of the complex.

er than the usual second derivative of dipole moment. This agrees with the fact that the ν_7–ν_8 combination has been observed to be very strong.[20]

B. Zeeman effect

While the detailed explanation of the observed values of $g_{\xi\xi}$ required *ab initio* calculation and is beyond the scope of this paper, we can explain some features of the values qualitatively. The negative values of g_{aa} and g_{bb} determined in this work show that the negative electronic contribution to the rotational magnetic moment given in the second term of Eq. (20) is larger than the positive nuclear contribution as for the case of H_2CO. This is understandable because the π electrons in the C≡C double bond give a large contribution to the magnetic moment. They do not produce a large magnetic moment by rotation around the c axis as indicated by the positive value of g_{cc}. This is quite different from the case of H_2CO in which the nonbonding lone pair electrons produce a large magnetic moment and make g_{cc} negative.

The relative values of g_{cc} for ethylene and formaldehyde can be semiquantitatively explained using a crude model. The first term of Eq. (20) for g_{aa} caused by the rotation of protons around the a axis is unity both for ethylene and formaldehyde because the factor of 2 for the number of protons is cancelled by the factor of 2 of the moment of inertia in the denominator. This means that the electronic contribution to g_{aa} is −1.42 for ethylene and −3.90 for formaldehyde. Since the moment of inertia I_{aa} for ethylene is about twice of that for formaldehyde, this means that the ratio of the values of $\Sigma'[|\langle 0|\hat{L}_a|n\rangle|^2/E_0 - E_n]$ for ethylene and formaldehyde is 11:15 indicating that the bonding π electrons contribute to the magnetic moment along a axis more than the nonbonding lone pair electrons.

ACKNOWLEDGMENTS

We are grateful to A. Fayt for sending us accurate molecular constants of ethylene in the ν_8 state. This work was supported in part by the Louis Block Fund of The University of Chicago, and also by the donors of the Petroleum Research Fund administered by the American Chemical Society.

[1] K. B. MacAdam and N. F. Ramsey, Phys. Rev. A **6**, 898 (1972).
[2] S. Gustafson and W. Gordy, Phys. Lett. A **49**, 161 (1974).
[3] D. W. Callahan, A. Yokozeki, and J. S. Muenter, J. Chem. Phys. **72**, 4791 (1980).
[4] T. E. Gough, B. J. Orr, and G. Scoles, J. Mol. Spectrosc. **99**, 143 (1983).
[5] N. J. Harrick and N. F. Ramsey, Phys. Rev. **88**, 228 (1952), etc., see the review by W. H. Flygare and R. C. Benson, Mol. Phys. **20**, 225 (1971), and references therein.
[6] S. G. Kukolich, P. D. Aldrich, W. G. Read, and E. J. Campbell, J. Chem. Phys. **79**, 1105 (1983).
[7] Y. T. Chen, J. M. Frye, and T. Oka, J. Opt. Soc. Am. B **3**, 935 (1986).
[8] C. J. Borde, Rev. Cethedec-Ondes et Signal NS 83-1, 1 (1983); G. Guelachvili and K. N. Rao, *Handbook of Infrared Standards* (Academic, New York, 1986).
[9] J. H. Van Vleck, Phys. Rev. **33**, 467 (1929).
[10] C. H. Townes and A. L. Schawlow, *Microwave Spectroscopy* (Dover, New York, 1975).
[11] J. R. Eshbach and M. W. P. Strandberg, Phys. Rev. **85**, 24 (1952); **82**, 237 (1951).
[12] Ch. Lambeau, A. Fayt, J. L. Duncan, and T. Nakagawa, J. Mol. Spectrosc. **81**, 227 (1980); A. Fayt (private communication).
[13] T. K. Bose and R. H. Cole, J. Chem. Phys. **54**, 3829 (1971).
[14] M. P. Bogaard and B. J. Orr, in *International Review of Science, Physical Chemistry, Series Two*, edited by A. D. Buckingham (Butterworths, London, 1975), Vol. 2, pp. 149–194.
[15] G. W. Hills and W. J. Jones, J. Chem. Soc. Faraday Trans. 2 **71**, 812 (1975).
[16] W. Hüttner, M.-K. Lo, and W. H. Flygare, J. Chem. Phys. **48**, 1206 (1968).
[17] R. C. Golike, I. M. Mills, W. B. Person, and B. Crawford, J. Chem. Phys. **25**, 1266 (1956).
[18] G. Jalsovszky and P. Pulay, J. Mol. Struct. **26**, 277 (1975).
[19] A. Komornicki and J. W. McIver, Jr., J. Chem. Phys. **70**, 2014 (1979).
[20] G. Herzberg, *Infrared and Raman Spectra of Polyatomic Molecules* (Van Nostrand, New York, 1945).